

Preliminary Design of a Test Rig for Combining Passive Nonlinear Isolation with Active Control

Muhajir AB RAHIM*, Timothy WATERS, Emiliano RUSTIGHI

Institute of Sound and Vibration Research,
University of Southampton, SO17 1BJ United Kingdom,
mar2g09@soton.ac.uk, tpw@isvr.soton.ac.uk, er@isvr.soton.ac.uk

ABSTRACT

Resilient elements are typically used to isolate delicate equipment from a vibrating host structure. Conventionally, these isolators are designed to operate in their linear region, but more recently nonlinear isolators have been employed to increase the frequency over which vibration isolation can be achieved. Another way of improving the performance of an isolator has been to use active control in conjunction with a passive linear system. The work presented in this paper concerns the development of an experimental rig for vibration isolation and is motivated by the intention to combine the advantages of passive nonlinear isolation with active control.

The structure consists of a mass suspended on four tensioned wires to form a single-degree-of-freedom system. The nonlinear stiffness of the wires is such that the system behaves like a hardening Duffing oscillator. Firstly, a static analysis is carried out, both analytically and experimentally, where the nonlinearity of the system is determined by the tension, length, cross-sectional area and Young's modulus of the wires. For the dynamic analysis, harmonic base excitation is considered. The magnitude of the base displacement is fixed for all excitation frequencies and the level of nonlinearity is adjusted by varying the tension in the wires, a higher tension leading to a milder system nonlinearity. Finally, the motion transmissibility of the system is measured and appears to agree with the theoretical result. The rig forms a suitable platform for subsequent incorporation of an active control system for combining the benefits of passive nonlinear isolation with, for example, skyhook damping.

Keywords: *nonlinear isolator, Duffing oscillator, harmonic base excitation*

1 INTRODUCTION

In many engineering structures, undesirable vibrations are a major concern. If uncontrolled, they can affect the performance and efficiency of the engineering applications. Traditionally, a linear passive isolator is employed to attenuate undesired vibration. The stiffness of the isolator is designed to be soft in order to have a wider isolation region [1]. However, in many practical situations a linear passive isolator has the issue of static deflection. This is because the mounted isolator cannot support the static load if the spring stiffness is too soft. To overcome this limitation, nonlinear stiffness isolators have been introduced [2,3]. In this design, the isolator is made to have a high-static-low-dynamic stiffness (HSLDS) so that it can support a large static load, while having low dynamic stiffness. Therefore, the system will have a low natural frequency such that a greater frequency range of vibration isolation can be achieved.

An HSLDS isolator can be achieved by combining a positive stiffness spring in parallel with a negative stiffness spring [2,3,4,5] or by geometrical nonlinearity [6]. In some cases, the resulting system can be described by the Duffing equation (provided that the motion is not excessive [7]), which is well known and understood [8,9]. A good review on recent advances in nonlinear passive isolator has been reported by Ibrahim [10].

A linear passive isolation system also has a trade-off in the choice of damping since good isolation at high frequencies requires a low level of damping whereas isolation at the fundamental mounted resonance frequency requires a high level of damping. Karnop [11] introduced the concept of skyhook damping to resolve this problem. Practically, this can be achieved by active control, whereby an actuator is placed in parallel with the linear passive isolator. Therefore, the control force which is supplied by the actuator will help to reduce the vibration at resonance, but without affecting performance at high frequencies [12-15].

There have been some studies, although perhaps surprisingly few, that have combined a nonlinear isolator with active control. For example, a study on the design of a tunable stiffness vibration isolator has been reported in [16]. In that study, a structural beam with a hardening stiffness property has been incorporated with a pair of electromagnets. As a result, the tunability of its stiffness is determined by the current supply to the electromagnets. By using the same model, an adaptive fuzzy-neural network controller has been applied to achieve active vibration control of the nonlinear isolator [17].

A lightly damped nonlinear isolator has the potential disadvantage of exhibiting the jump up and jump down phenomenon in which the level of response can jump between two stable solutions when, for example, the frequency of excitation is slowly varied in the vicinity of resonance. The implementation of active damping control such as skyhook damping can in principle be employed to overcome this issue whilst not affecting high frequency isolation. This is the eventual goal of the work presented.

The main objective of this paper is to describe the design and construction of a rig that behaves like a Duffing oscillator that features symmetric nonlinear stiffness but is also amenable to active control. The structure of this paper starts in section 2 with the theory of motion transmissibility for an isolator modelled as a Duffing oscillator, which is derived using the harmonic balance method. The equations of motion for the static response of the practical system comprising four tensioned wires is then presented which enables the system to be represented in Duffing form. Section 3 provides a brief description of the experimental rig. Section 4 presents a comparison of the experimental and theoretical results for first the static response and then the motion transmissibility. Finally, modifications to the rig to facilitate active control are discussed.

2 THEORETICAL ANALYSIS

2.1 Motion transmissibility of a Duffing oscillator

Figure 1 depicts a simple schematic diagram of a single-degree-of-freedom (SDOF) base-excited Duffing oscillator. It consists of a mass m which is mounted on hardening stiffness (for positive k_3) and a constant damping coefficient c . The motion of the base and the displacement of the mass are given as $z = Z\cos(\omega t)$ and $x = X\cos(\omega t + \vartheta)$ respectively. Z is the amplitude of the base excitation, X is the displacement amplitude of the mass, ω is the excitation frequency, ϑ is the phase, and t is time.

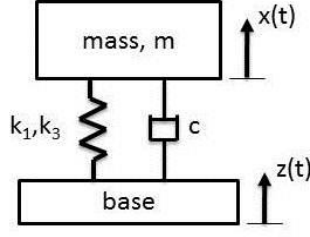


Figure 1-Single-degree-of-freedom model of a nonlinear isolator

The equation of motion of the system can be written in the form of Duffing's equation as

$$m\ddot{u} + c\dot{u} + k_1u + k_3u^3 = -m\ddot{z} \quad (1)$$

where k_1 is the linear stiffness, k_3 is cubic stiffness, c is viscous damping, and $u=x-z$, is the relative displacement between the mass and the base. Eq. (1) can be nondimensionalised to become

$$\hat{u}'' + 2\zeta\hat{u}' + \hat{u} + \alpha\hat{u}^3 = \Omega^2\cos(\Omega\tau) \quad (2)$$

where:

$$\zeta = \frac{c}{2m\omega_n} \quad \omega_n^2 = \frac{k_1}{m} \quad \alpha = \frac{k_3Z^2}{k_1} \quad \Omega = \frac{\omega}{\omega_n} \quad \tau = \omega_n t$$

$$\hat{u}'' = \frac{\ddot{u}}{\omega_n^2 Z} \quad \hat{u}' = \frac{\dot{u}}{\omega_n Z} \quad \hat{u} = \frac{u}{Z}$$

with the symbol “/” denoting differentiation with respect to nondimensional time τ . Note that α is a factor that determines the degree of nonlinearity of the system. Therefore, the nonlinearity α in this system takes into account the magnitude of the base excitation Z , the linear stiffness k_1 and the cubic stiffness k_3 . It is clear that the system defaults to a linear system if $\alpha = 0$.

The solution of Eq. (2) can be attained through analytical and numerical methods, as for example reported in [18]. In this study the Harmonic Balance (HB) method is applied because it is mathematically simple and not restricted to weakly nonlinear problem [19]. The solution of the HB method is based on the assumption that the response is harmonic at the excitation frequency, and can be expressed as

$$\hat{u} = \hat{U}\cos(\Omega\tau + \varphi) \quad (3)$$

where \hat{U} and φ are the amplitude and phase of the relative displacement with respect to the base motion.

By using the HB method the frequency response relating \hat{U} to the frequency ratio Ω can be obtained from

$$\frac{9}{16}\alpha^2\hat{U}^6 + \frac{3}{2}(1-\Omega^2)\alpha\hat{U}^4 + [(1-\Omega^2)^2 + 4\zeta^2\Omega^2]\hat{U}^2 = \Omega^4 \quad (4)$$

which can be alternatively expressed as

$$(\hat{U}^2 - 1)\Omega^4 + \left[(4\zeta^2 - 2)\hat{U}^2 - \frac{3\alpha}{2}\hat{U}^4 \right] \Omega^2 + \frac{9}{16}\alpha^2\hat{U}^6 + \frac{3}{2}\alpha\hat{U}^4 + \Omega^4 = 0 \quad (5)$$

By solving Eq. (5) for Ω yields two solutions,

$$\Omega_1 = \sqrt{\frac{3\alpha\hat{U}^4 + 4\hat{U}^2(1-2\zeta^2) - \hat{U}\sqrt{(3\alpha\hat{U}^2 + 4)^2 - 64\hat{U}^2\zeta^2(1-\zeta^2)} - 48\alpha\zeta^2\hat{U}^4}{4(\hat{U}^2 - 1)}} \quad (6)$$

$$\Omega_2 = \sqrt{\frac{3\alpha\hat{U}^4 + 4\hat{U}^2(1-2\zeta^2) + \hat{U}\sqrt{(3\alpha\hat{U}^2 + 4)^2 - 64\hat{U}^2\zeta^2(1-\zeta^2)} - 48\alpha\zeta^2\hat{U}^4}{4(\hat{U}^2 - 1)}}$$

of which only the real solutions, where they exist, are of interest. Note that, \hat{U} is the relative transmissibility. However, the absolute transmissibility is usually of more interest in defining the performance of an isolator, i.e. the ratio of displacement of the mass to the base, and is given by

$$|T_a| = \sqrt{1 + 2\hat{U}\cos\varphi + \hat{U}^2} \quad (7)$$

where, from HB method, $\cos\varphi$ is given by

$$\cos\varphi = \frac{\left(1 - \Omega^2 + \frac{3}{4}\alpha U^2\right)U}{\Omega^2} \quad (8)$$

By substituting Eq. (8) into Eq. (7), the absolute motion transmissibility can be expressed as

$$|T_a| = \sqrt{1 + \hat{U}^2 + \frac{2\hat{U}^2}{\Omega^2}\left(1 - \Omega^2 + \frac{3}{4}\alpha U^2\right)} \quad (9)$$

2.2 System Modelling

The proposed nonlinear isolator in this work is illustrated in Figure 2. It comprises an isolated mass m which is attached to four radially orientated wires of initial length $L/2$ and tension T . For clarity, only two wires are shown.

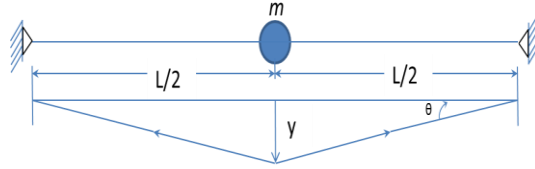


Figure 2- Model of a Duffing oscillator comprising a mass suspended on tensioned wires

When the mass moves in the y direction, the corresponding strain ε in each wire can be expressed as

$$\varepsilon = \frac{\sqrt{L^2/4 + y^2} - L/2}{L/2} \quad (10)$$

As a consequence, the total tension in each wire is $(T + AE\varepsilon)$, where A and E are the cross section area and the modulus of elasticity of the wire respectively.

Since there are four wires subtending the same angle θ to the horizontal, the applied force on the mass m in the y direction is related to angular deflection as

$$f = 4(T + AE\varepsilon)\sin\theta \quad (11)$$

where

$$\sin\theta = \frac{y}{\sqrt{L^2/4 + y^2}} \quad (12)$$

By using a Taylor-series expansion to the third order and by assuming the displacement y to be small compared with L , Eq. (12) can be written as

$$\sin\theta = \frac{2y}{L} - \frac{4y^3}{L^3} \quad (13)$$

By substituting Eq.(10) and Eq.(13) into Eq. (11), the relationship between the applied static force and the resulting displacement y can be expressed as

$$f = \frac{8T}{L}y + \frac{16AE}{L^3}\left(1 - \frac{T}{AE}\right)y^3 \quad (14)$$

It is clear that the linear and cubic stiffness coefficients of this Duffing oscillator are given by

$k_1 = \frac{8T}{L}$ and $k_3 = \frac{16AE}{L^3}\left(1 - \frac{T}{AE}\right)$ respectively. From these two known analytical expressions and

the magnitude of the base excitation, the nonlinearity of the system is determined, since $\alpha=(k_3/k_1)Z^2$. By assuming that $T/AE \ll 1$, it becomes apparent that a higher tension will produce a higher linear stiffness k_1 , whilst having a negligible effect on k_3 and so will give a lower nonlinearity for a given base motion Z .

3 DESCRIPTION OF THE DESIGNED RIG

The design of the oscillator is based on several requirements. Firstly, it is required to behave as a single-degree-of-freedom system over a sufficiently wide bandwidth to demonstrate the expected behaviour from the model. Secondly, it must have a symmetrical hardening characteristic. This indicates that the stiffness of the system must increase similarly in both directions as it oscillates from the equilibrium position. Thirdly, the natural frequency of the linearized system is preferred to be approximately at 15 Hz. This is to avoid the possibility of interaction between the resonances of the structure and the shaker when the structure's natural frequency is close to that of the shaker, as reported in [20]. Finally, the designed system must be lightly damped in order to demonstrate the benefits of active control, for example in the implementation of skyhook damping.

In order to meet these requirements, a model with an isolated mass which is suspended by four stretched wires is designed in a symmetric arrangement, as shown in Figure 3. The isolated mass is designed as a disc shape with a mass of 0.08kg, and made from aluminium. A nylon fishing line is used as the wire. The isolated mass is suspended by the wires between four pillars which are placed on a supposedly rigid aluminium foundation base, with dimensions of 0.158m x 0.158m x 0.01m. The length of each wire is 0.07m, and the tension of each wire is adjustable.

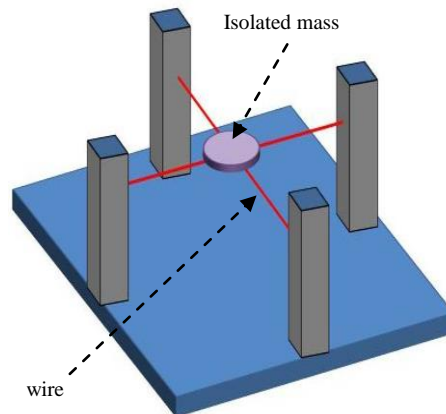


Figure 3- The experimental test rig designed to behave like a hardening Duffing oscillator

4 EXPERIMENTAL STUDIES

4.1 Static Test

Firstly, a static test was carried out by directly measuring the static displacement with a laser sensor due to an applied static force. Measurements were repeated three times and an average taken. In this study, the test rig was placed horizontally to avoid gravitational effects. In order to observe the effect of tension in the wire, two different initial tensions were considered. In the first experiment, all the wires were adjusted to have similarly low initial tension. Meanwhile, high tensions were applied in the wires for the second experiment. Figure 4 shows the averaged experimental results of force-displacement for these two different initial tension values. In the figure, the dots represent the measured values of the first experiment, and circles represent the measured values for the second experiment. The solid and dashed lines are the approximate cubic function curve fits for the first and second experiment respectively. It is reasonably convincing that

the static behaviour of the system is consistent with the cubic stiffness assumption of a Duffing oscillator over this displacement range. The expression for the curve fit for the first experiment is $f_1=380.7y + 2 \times 10^7 y^3$. Therefore, the linear and cubic stiffness in the first experiment can be assumed to be $k_1=380.7$ N/m and $k_3=2 \times 10^7$ N/m³ respectively. Meanwhile, the best-fit force-displacement relationship for the second experiment is $f_2=760.4y + 2 \times 10^7 y^3$, where $k_1=760.4$ N/m and $k_3=2 \times 10^7$ N/m³.

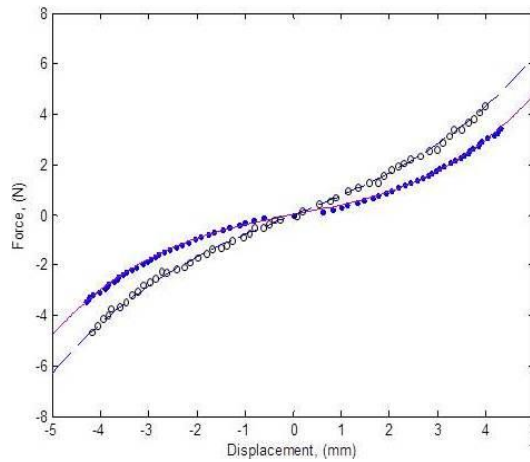


Figure 4- Force-displacement plot of the designed test rig. The measured values (dots) and best-fit curve (solid line) for the first experiment; the measured values (circles) and the best-fit curve (dashed line) for second experiment.

4.2 Dynamic Test

The dynamic test in this study considers motion transmissibility. The test rig was mounted on a VP4 Derritron shaker in the horizontal position as shown in Figure 5, and the setup of the test equipment is illustrated in Figure 6. The acceleration of the isolated mass and the base excitation of the shaker were measured by PCB 352C22 accelerometers. Initially, a measurement of the frequency response function of the ‘linear’ system was conducted using a low level pseudo random excitation signal, and the Frequency Response Function (FRF) of the system was estimated using the H1 estimator. The FRFs are not shown here for brevity but the natural frequencies were observed to be at 10.8 Hz for the first experiment (low tension) and 16 Hz for second experiment (higher tension).

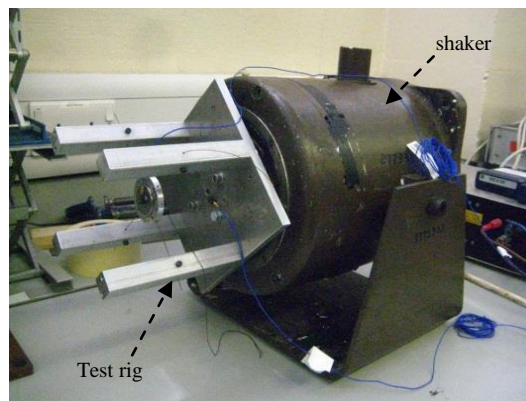


Figure 5- The designed test rig attached to the shaker in a horizontal position

Figure 7 presents the experimental setup for the system nonlinear measurement. The harmonic base excitation was varied manually, using a signal generator, from 10Hz to 20Hz in increasing steps of 1Hz, and also from 20Hz to 10Hz in decreasing steps of 1Hz. The gain was adjusted manually at each frequency in turn to ensure a base excitation Z of amplitude 1.5×10^{-4} m

for both of experiments (low and high tension). With the linear and cubic stiffnesses previously obtained the nonlinearity of the system in the first and second experiments is expected to be given by $\alpha_1=1.18 \times 10^{-3}$ and $\alpha_2=5.92 \times 10^{-4}$ respectively.

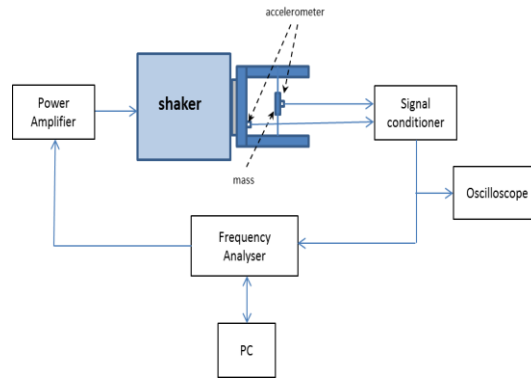


Figure 6- Experimental setup for frequency response function test.

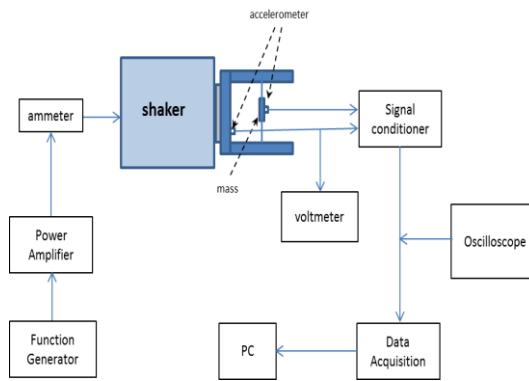


Figure 7- Experimental setup for nonlinear measurement.

The motion transmissibility measurement is determined by the ratio of the root-mean-square (rms) voltage of the isolated mass to the rms voltage of the base for each excitation frequency. Figures 8(a) and (b) show the experimental result for the first (low tension) and second experiment (high tension) respectively. The data points in each graph are denoted by ‘.’ for increasing frequency and ‘+’ for decreasing frequency. The dashed lines represent the analytical results assuming the estimated values of α given above. The behaviour is qualitatively similar, with both theory and experiment exhibiting the jump up and jump down phenomenon. However, the nonlinearity is less exaggerated in the experiment. The solid lines in the figures pertain to analytical results obtained when adopting lower values of α ($\alpha_1=5.25 \times 10^{-4}$ and $\alpha_2=2.50 \times 10^{-4}$) that best fit the experimental data.

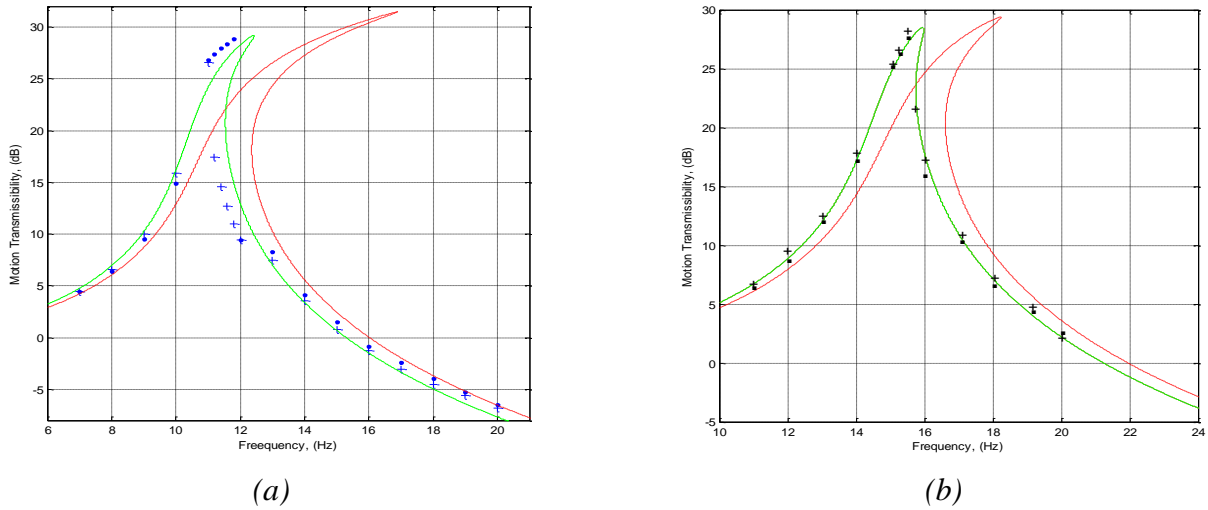


Figure 8- Analytical and experimental result of nonlinear motion transmissibility for (a) the wire with low tension and (b) the wire with high tension. The measured values with increasing frequency ('.'), measured values with decreasing frequency ('+'), the analytical results with previously estimated values of α (dashed line) and analytical results with α chosen to give the best fit (solid line).

4.3 Further rig development

Two modifications will be made to the test rig, as illustrated in Figure 9. Firstly is the application of load cells such that the tensions in the wires can be measured and carefully controlled. Secondly is the employment of a voice coil actuator to implement active skyhook damping. The coil will be mounted on the isolated mass and suspended within the magnetic field provided by a permanent magnet fixed to the base. The stiffness of the system will be unaffected by this non-contacting arrangement. A reasonably large air gap may be required to accommodate any unintentional rocking motion of the mass and coil.

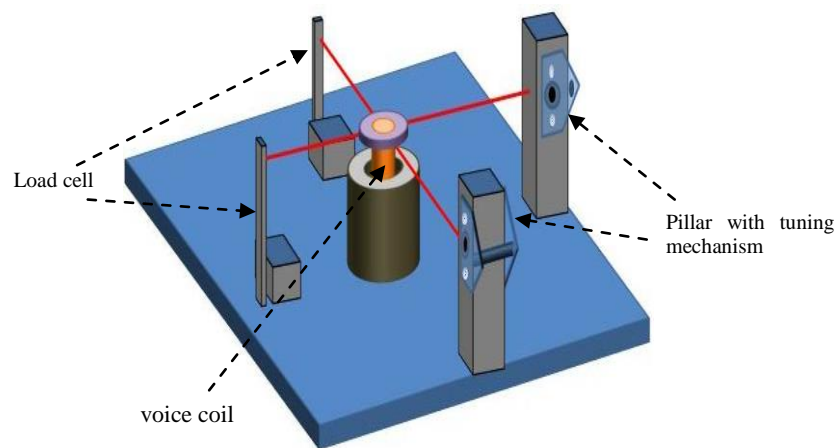


Figure 9- The proposed test rig design for active control of the nonlinear isolation system

5 CONCLUSIONS

In this paper, a design has been presented for a nonlinear isolator system with hardening stiffness. A static test has been performed to measure its force deflection characteristics and this is seen to resemble theory closely. The motion transmissibility of the system has also been measured which exhibits clear nonlinear behaviour that is consistent with that obtained from theory using the harmonic balance method. This behaviour is undesirable and can, in principle, be ameliorated without deterioration of isolation at high frequencies by adding skyhook damping. The rig is being modified in order to demonstrate the benefits of combining active damping with a passive nonlinear mount.

REFERENCES

- [1] W. Thomson, *The Theory of Vibration with Applications*. 1996: Taylor & Francis; New ed of 4 Revised edition.
- [2] A. Carrella, *Passive Vibration Isolators with High-Static-Low-Dynamic-Stiffness*, PhD Thesis. 2008, University of Southampton.
- [3] P. Alabuzhev, P.M. Alabuzhev, E.I. Rivin, *Vibration protecting and measuring systems with quasi-zero stiffness*. 1989: Hemisphere Pub. Corp.
- [4] T. Mizuno, M. Takasaki, D. Kishita, K. Hirakawa, *Vibration isolation system combining zero-power magnetic suspension with springs*. Control Engineering Practice, 2007. **15**(2) p. 187-196.
- [5] D. Platus, *Negative-stiffness-mechanism vibration isolation systems*. in *Proceedings of SPIE, Vibration Control in Microelectronics, Optics, and Metrology 161*. 1992.
- [6] L.N. Virgin, S.T. Santillan, R.H. Plaut, *Vibration isolation using extreme geometric nonlinearity*, in *Euromech Colloquium 483 Geometrically Non-linear Vibrations of Structures*. 2007: Porto, Portugal.
- [7] I. Kovacic, M.J. Brennan., *The Duffing Equation: Nonlinear Oscillators and Their Behaviour*. 2011: John Wiley & Sons.
- [8] A.H. Nayfeh, D.T. Mook, *Nonlinear oscillations*. 1979: Wiley.
- [9] J.J. Stoker, *Nonlinear Vibrations in Mechanical and Electrical Systems*. 1950: Interscience Publisher Ltd.
- [10] R.A. Ibrahim, *Recent advances in nonlinear passive vibration isolators*. Journal of Sound and Vibration, 2008. **314**: p. 371-452.
- [11] D.C. Karnopp, M.J. Crosby, R.A. Harwood, *Vibration Control Using Semi-Active Force Generators* J. Eng. Ind. , 1974. **96**: p. 619–626.
- [12] C.R. Fuller, S.J. Elliott, P.A. Nelson, *Active control of vibration*. 1996: Academic Press, New York, 1996.

- [13] S.M. Kim, S.J. Elliott, M.J. Brennan, *Decentralised control for multichannel active vibration isolation*. *IEEE Transactions on Control Systems Technology*, 9, (1), p. 93-100
- [14] X. Huang, S.J. Elliott, M.J. Brennan, *Active isolation of a flexible structure from base vibration*. *J. Sound Vib.*, 2003. **263**.
- [15] M. Serrand, S.J. Elliott, *Multichannel feedback control for the isolation of base-excited vibration*. *J. Sound Vib.*, 2000. **234**.
- [16] N. Zhou, K. Liu, *A tunable high-static–low-dynamic stiffness vibration isolator*. *Journal of Sound and Vibration*, 2010. **329**(9): p. 1254-1273.
- [17] N. Zhou, *A Tunable High-Static–Low-Dynamic-Stiffness Isolator and Fuzzy-Neural Network Based Active Control Isolator*, M.Sc. Thesis, Lakehead University, 2009.
- [18] M.J. Brennan, I. Kovacic, A. Carrella, T.P. Waters, *On the jump-up and jump-down frequencies of the Duffing oscillator*. *Journal of Sound and Vibration*, 2008. **318**(4-5): p. 1250-1261.
- [19] M.N. Hamdan, T.D. Burton, *On the Steady State Response and Stability of Non-Linear Oscillators Using Harmonic Balance*. *Journal of Sound and Vibration*, 1993. **166**(2): p. 255-266.
- [20] G. Gatti, I. Kovacic, M.J. Brennan, *On the response of a harmonically excited two degree-of-freedom system consisting of a linear and a nonlinear quasi-zero stiffness oscillator*. *Journal of Sound and Vibration*, 2010. **329**(10): p. 1823-1835.